# Transport of Viruses Through Saturated and Unsaturated Columns Packed with Sand

**Robert Anders · Constantinos V. Chrysikopoulos**

**Abstract**    Laboratory-scale virus transport experiments were conducted in columns packed with sand under saturated and unsaturated conditions. The viruses employed were the male-specific RNA coliphage, MS2, and the *Salmonella typhimurium* phage, PRD1. The mathematical model developed by Sim and Chrysikopoulos (Water Resour Res 36:173–179, 2000) that accounts for processes responsible for removal of viruses during vertical transport in one-dimensional, unsaturated porous media was used to fit the data collected from the laboratory experiments. The liquid to liquid–solid and liquid to air–liquid interface mass transfer rate coefficients were shown to increase for both bacteriophage as saturation levels were reduced. The experimental results indicate that even for unfavorable attachment conditions within a sand column (e.g., phosphate-buffered saline solution; pH = 7.5; ionic strength = 2 mM), saturation levels can affect virus transport through porous media.

**Keywords**    Bacteriophage · Virus transport · Unsaturated flow · Virus inactivation · Interface mass transfer · Mathematical modeling

## Notations

$a_T$     Specific liquid–solid interface area, $L^2/L^3$
$a_T^\diamond$     Specific air–liquid interface area, $L^2/L^3$
$b$     Empirical constant
$C$     Virus concentration in liquid phase, $M/L^3$
$C_0$     Pulse-type source concentration, $M/L^3$

R. Anders (✉)
U.S. Geological Survey, 4165 Spruance Rd., Ste. 200, San Diego, CA 92101, USA
e-mail: randers@usgs.gov

R. Anders
Department of Civil and Environmental Engineering, University of California, Irvine, CA 92697, USA

C. V. Chrysikopoulos
Department of Civil Engineering, University of Patras, Patras 26500, Greece
e-mail: gios@upatras.gr

$C^*$     Deposited virus concentration at the liquid–solid interface
       (virus mass/solid mass), M/M

$C^\diamond$     Absorbed virus concentration at the air–liquid interface, $M/L^3$

$C_g$     Concentration of viruses in direct contact with solids, $M/L^3$

$d_v$     Virus diameter, L

$\mathcal{D}$     Molecular diffusion coefficient, $L^2/t$

$\mathcal{D}_e$     Effective molecular diffusion coefficient, $L^2/t$

$D_z$     Vertical hydrodynamic dispersion coefficient, $L^2/t$

$g$     Gravitational constant, $L/t^2$

$h$     Soil water pressure head, L

$h_0$     Air-entry value, L

$k$     Liquid to liquid–solid interface mass transfer rate coefficient, $t^{-1}$

$k_B$     Boltzman constant, $(ML^2)/(t^2\,T)$

$k^\diamond$     Liquid to air–liquid interface mass transfer rate coefficient, $t^{-1}$

$K$     Unsaturated hydraulic conductivity, L/t

$K_d$     Partition or distribution coefficient, $L^3/M$

$m$     Empirical constant

$n$     Empirical constant

$q$     Specific discharge (Darcian fluid flux), L/t

$q_0$     Prescribed specific discharge, L/t

$r_0$     Effective pore radius at air entry, L

$r_p$     Average radius of soil particles, L

$S_e$     Effective degree of saturation

$t$     Time, t

$t_p$     Duration of source pulse, t

$U$     Average interstitial velocity, ($U = q/\theta_m$), L/t

$z$     Spatial coordinate in vertical direction, L

*Greek Letters*

$\alpha$     Empirical coefficient, $L^{-1}$

$\alpha_z$     Vertical dispersivity, L/t

$\zeta$     Empirical coefficient

$\theta_m$     Moisture content (liquid volume/porous medium volume), $L^3/L^3$

$\theta_r$     Residual or monolayer volumetric moisture content, $L^3/L^3$

$\theta_s$     Volumetric water content of a saturated porous medium, $L^3/L^3$

$\kappa$     Liquid to liquid–solid interface mass transfer coefficient, L/t

$\kappa^\diamond$     Liquid to air–liquid interface mass transfer coefficient, L/t

$\lambda$     Inactivation rate coefficient of suspended viruses, $t^{-1}$

$\lambda^*$     Inactivation rate coefficient of sorbed viruses at the liquid–solid interface, $t^{-1}$

$\lambda^\diamond$     Inactivation rate coefficient of sorbed viruses at the air–liquid interface, $t^{-1}$

$\mu$     Viscosity of the liquid, $M/(L\,t)$

$\rho$     Bulk density of the solid matrix (solids mass/aquifer volume), $M/L^3$

$\rho_w$     Density of water, $M/L^3$

$\sigma$     Surface tension of water, $M/t^2$

$\tau$     Tortuosity ($\tau \geq 1$)

**Abbreviations**

ATCC    American type culture collection
PBS     Phosphate buffered saline
PFU     Plaque forming units
SSE     Sum of squared error
TSA     Trypticase soy agar
TSB     Trypticase soy broth

## 1 Introduction

Virus contamination can originate from a number of different sources, including landfills, septic tanks, and recharge basins (National Research Council 1994). In each of these cases, the viruses would travel through the unsaturated zone before reaching the ground water. The major processes controlling the transport of viruses in the subsurface are sorption and/or inactivation (Gerba and Keswick 1981; Chrysikopoulos and Sim 1996). The degree of virus attachment is affected by several factors including viral surface properties, groundwater quality, and sediment surface charges (Gerba 1984). Lance and Gerba (1984) reported that a reduction in soil moisture content enhances virus sorption by forcing viruses to move into a thin film of water surrounding soil particles. Other investigators have noted that virus sorption is strongly correlated with the degree of soil moisture due to the presence of solid–water and air–water interfaces in unsaturated porous media (Powelson et al. 1990; Wan and Wilson 1994). By conducting well-controlled studies under unsaturated conditions, Jin et al. (2000) contributed the presence of an air–water interface for the observed increase in the removal of two bacteriophage. Chu et al. (2001) suggested that in the absence of a reactive solid–water interface the reactions at the air–water interface may become more pronounced and accentuated at low water contents.

The inactivation of viruses is enhanced due to the presence of an air–liquid interface (Thompson et al. 1998). Thompson and Yates (1999) suggested that the presence of air–liquid–solid interfacial forces increased the inactivation of a relatively hydrophobic virus in tubes composed of hydrophobic solid surfaces but not in tubes composed of hydrophilic solid surfaces. However, there is no quantitative relationship between the inactivation rate coefficients of viruses in the liquid phase and viruses sorbed at the air–liquid interface available in the literature. Given that the presence of air–water interfaces may serve as sorption sites for viruses and enhance inactivation, an attempt to predict the degree of virus attenuation during vertical transport through unsaturated soil requires a relationship among moisture content, sorption, and inactivation of viruses at the air–liquid interface as well as at the solid–liquid interface.

For this work, laboratory-scale transport experiments were conducted in packed sand columns under saturated and unsaturated conditions using: (1) the male-specific RNA coliphage MS2; (2) the *Salmonella typhimurium* phage, PRD1; and (3) bromide as the nonreactive tracer. The mathematical model developed by Sim and Chrysikopoulos (2000) to quantify the processes responsible for removal of viruses during vertical transport in one-dimensional, unsaturated porous media was used to obtain the liquid to liquid–solid and liquid to air–liquid interface mass transfer rate coefficients corresponding to the data collected from the laboratory experiments. The ability to more accurately predict the transport of viruses in saturated and unsaturated porous media using interface mass transfer rate coefficients normalized by the specific liquid–solid and air–liquid interface areas is discussed.

## 2 Materials and Methods

2.1 Bacteriophage Assays

The model viruses employed for this study were MS2 and PRD1. MS2 is an icosahedral, single-stranded RNA male-specific coliphage with an average diameter of $\sim 25$ nm and an isoelectric point ($pH_{iep}$) of 3.9 (Zerda 1982). PRD1 is an icosahedral, double-stranded DNA somatic *Salmonella typhimurium* phage, 62 nm in diameter, with $pH_{iep} \sim 4.5$ measured in a calcium phosphate buffer solution containing $10^{-4}$ M calcium (Bales et al. 1991). These bacteriophage have been used extensively in virus transport and inactivation studies and are considered to be good model viruses because they behave more conservatively (attach poorly) than many pathogenic viruses and are relatively persistent during transport through the subsurface (Hurst et al. 1980; Yates et al. 1985; Yahya et al. 1993; Bales et al. 1997; Ryan et al. 1999, 2002; Schijven et al. 1999; Harvey and Ryan 2004; Keller et al. 2004; Anders and Chrysikopoulos 2005; Masciopinto et al. 2008).

The effluent concentrations of each bacteriophage were measured using the single-agar-layer assay method (U.S. Environmental Protection Agency 2001). Trypticase soy broth (TSB) (Difco), TSB (Difco) soft agar (containing 0.05% 1 N CaCl$_2$) and trypticase soy agar (TSA) (Difco) bottom agar were used for analyzing PRD1 bacteriophage using *Salmonella typhimurium* LT2 (ATCC #15277) as the host bacterium. For the analysis of MS2 bacteriophage, *E. coli* F$^-$ amp (ATCC #700981) were used as the host bacterium with the same concentration of antibiotics as described by Debartolomeis and Cabelli (1991). In order to ensure that all host bacteria were in log-phase growth, 0.1 ml of prepared stocks of each host were transferred to a test tube containing 10 ml of TSB and placed in a shaker at 37°C for 4 h or until cultures were visibly turbid. The mixture was gently mixed and poured onto the appropriate plating medium. The plates were incubated at 37°C for 24 h. The virus concentrations were determined by counting the number of circular lysis zones (plaques) on each plate. Plates were made in duplicate and the concentrations were averaged from the plaques counted on each plate. Following Method 1602 of the U.S. Environmental Protection Agency (2001), the single-agar-layer assay used in this study was estimated to have a detection limit of 0.5 plaque forming units (PFU)/ml.

2.2 Bromide Analysis

Bromide, in the form of potassium bromide, was chosen as the nonreactive tracer for the transport column experiments. The nonreactive tracer solution was prepared with 0.6 mM KBr in water purified to a specific conductance of 17.8 µS/cm with a Milli-Q UV plus water purification system (Millipore Corp., MA) containing a filter with 0.22 µm pore size and UV sterilization. It should be noted that alkali halides are the most commonly used salts for subsurface fluid tracing owing to a minimal effect on solution ionic strength (Chrysikopoulos 1993). All effluent samples for bromide were collected into borosilicate test tubes. Bromide concentrations were measured using ion chromatography (ICS-1500, Dionex Corp., Sunnyvale, CA).

2.3 Sand Preparation

Clean, graded, kiln-dried Monterey sand (RMC Industries, Decatur, GA) was used in this study. The mean diameter of the sand was determined to be approximately 250 µm. The sand was soaked in UV-disinfected distilled water for several days to remove any salts and

oven-dried for 24 h at 105°C. The sand was placed in sterile containers to reduce the possibility of microbial contamination.

Analysis by X-ray powder diffractometry found that the sieved sand is composed of quartz as the major phase (>25% by weight) with minor amounts (between 5 and 25% by weight) of microcline and albite and trace amounts (<5% by weight) of muscovite and phlogopite. Reflectance spectroscopic analysis with an Analytical Spectral Devices Full Range Spectrometer© over the visible to near-infrared wavelength range (0.4–2.5 µm) using a halogen lamp for illumination and Spectralon© panel for reference (Clark et al. 2007) identified hematite coatings on the grains. Total carbon was measured with a carbon analyzer (LECO, Model CR-412) and found to be less than 0.05 g/kg of sand (Taggart 2002).

### 2.4 Preparation of Virus Suspension

An aliquot of stock suspensions of both bacteriophage was diluted with a low-ionic-strength phosphate-buffered saline (PBS) solution. The PBS solution was prepared with 0.25 mM $Na_2HPO_4$, 1.2 mM NaCl, 0.037 mM KCl in UV-disinfected distilled water with a specific conductance of 17.8 µS/cm, and adjusted to a pH of 7.5 with HCl. The final virus suspension was prepared by combining the diluted stock suspensions with the nonreactive tracer. The resulting virus suspension contained bacteriophage MS2 and PRD1 concentrations of $5.0 \times 10^5$ and $5.5 \times 10^5$ PFU/ml, respectively. The specific conductance of the final virus suspension was 212 µS/cm, which corresponds to an ionic strength of about 2 mM.

### 2.5 Transport Experiments

The transport column experiments were conducted under saturated conditions and under decreasing levels of water saturation. For each experiment, the prewashed sand was dry-packed into 15.2 cm long Plexiglas© columns with 5.1 cm diameter. Several pore volumes of the de-aired PBS solution were passed through each column from the bottom at a rate of 1 ml/min to avoid the capture of air bubbles. The porosity and bulk density of each column were determined by noting the weight difference before and after each column was completely saturated with the PBS solution. Initial bacteriophage concentrations were measured from samples collected through the tubing before the tubing was attached to the column. The saturated transport experiments were conducted using the laboratory setup shown in Fig. 1. The virus suspension was introduced from the bottom of the column and effluent samples were collected from the top exit of the column.

For the unsaturated experiments, the packed columns were attached to the special apparatus shown in Fig. 2 that allowed for various levels of water saturation. The apparatus (Soil Measurement Systems, Tucson, AZ) includes a fraction collector, which is located inside a vacuum chamber. The packed column was placed above the vacuum chamber with its lower outlet connected to the vacuum chamber. The virus suspension was applied using a syringe pump in order to maintain the injection rates necessary to create a constant water potential throughout the packed column. The water potential was measured by tensiometers placed into the upper and lower ends of each packed column. The water potential values were recorded with a datalogger (Campbell Scientific, Inc., Logan, UT). Liquid samples were collected at regular time intervals from the column effluent in small fractions with the automatic fraction collector. The pressure inside the vacuum chamber was controlled by the pressure regulator and monitored by a hand-held tensiometer attached to the tensiometer port. The amount of water saturation for each column was determined by measuring the volumetric moisture content after each unsaturated experiment. It should be noted that the volumetric moisture
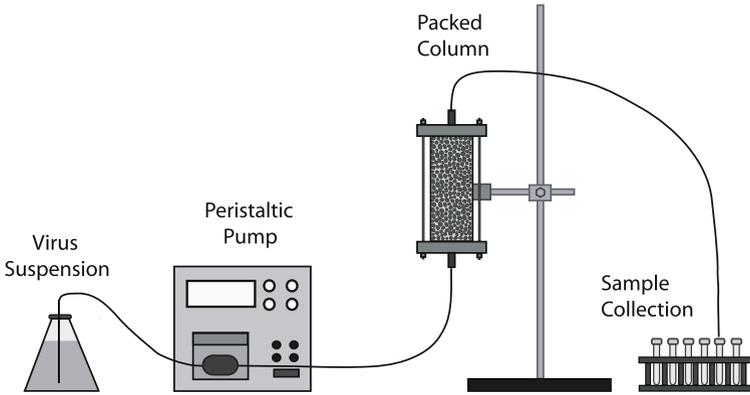
**Fig. 1** Schematic illustration of the experimental setup for column studies under saturated conditions
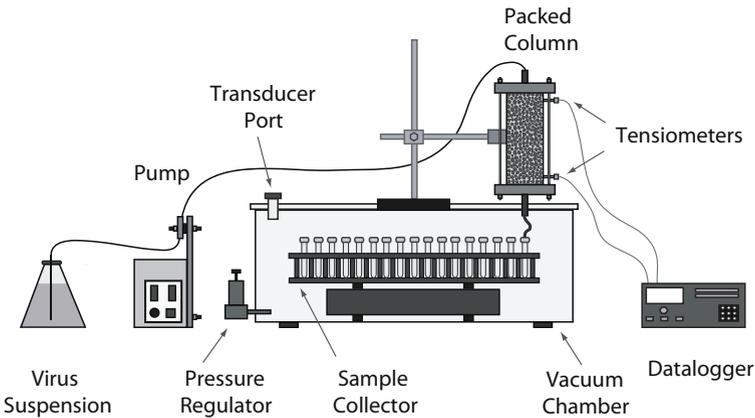


**Fig. 2** Schematic illustration of the experimental setup for column studies under unsaturated conditions

content is equal to the mass of water retained in the column divided by the total inner volume of the column (the initial volumetric moisture content is assumed equal to the porosity). Upon completion of each experiment, the Plexiglas$^{©}$ column apparatus was disassembled, cleaned, and reassembled.

## 3 Model Development

### 3.1 Virus Transport in Unsaturated Porous Media

The mathematical model originally presented by Sim and Chrysikopoulos (2000) that describes the transport of viruses in one-dimensional, unsaturated porous media, accounting for virus sorption and inactivation is governed by the following partial differential equation:

$$
\frac{\partial}{\partial t}(\theta_m C) + \rho \frac{\partial C^*}{\partial t} + \frac{\partial}{\partial t}(\theta_m C^\diamond) = \frac{\partial}{\partial z}\left(D_z \theta_m \frac{\partial C}{\partial z}\right) - \frac{\partial}{\partial z}(qC)
$$
$$
- \lambda \theta_m C - \lambda^* \rho C^* - \lambda^\diamond \theta_m C^\diamond, \tag{1}
$$

where $C$ is the virus concentration in the liquid phase; $C^*$ is the deposited virus concentration at the liquid–solid interface; $C^\diamond$ is the adsorbed virus concentration at the air–liquid interface; $q$ is the specific discharge (Darcian fluid flux); $\theta_m$ is the volumetric moisture content (moisture volume divided by the total volume of the porous medium); $\lambda$, $\lambda^*$, and $\lambda^\diamond$ are the inactivation rate coefficients of viruses suspended in the liquid phase, viruses sorbed at the liquid–solid interface, and viruses sorbed at the air–liquid interface, respectively; $\rho$ is the bulk density of the solid matrix; $t$ is time; and the vertical spatial coordinate $z$ is positive downward.

The vertical hydrodynamic dispersion coefficient $D_z$ is defined as (Nielsen et al. 1986):

$$D_z = \alpha_z \frac{q}{\theta_m} + \mathcal{D}_e, \tag{2}$$

where $\mathcal{D}_e = \mathcal{D}/\tau$ is the effective molecular diffusion coefficient in the unsaturated porous medium (where $\mathcal{D}$ is the molecular diffusion coefficient and $\tau \geq 1$ is the tortuosity coefficient); and $\alpha_z$ is the vertical dispersivity. The molecular diffusion coefficient is governed by Brownian motion and is described by the Stokes–Einstein equation as (Atkins 1990):

$$\mathcal{D} = \frac{k_B T}{3\pi \mu d_v}, \tag{3}$$

where $k_B = 1.38 \times 10^{-23}$ (kg m$^2$)/(s$^2$ K) is the Boltzmann constant, $d_v$ is the virus diameter, $\mu = 8.91 \times 10^{-4}$ kg/(m s) is the viscosity of water, and $T$ is the absolute temperature in Kelvin. The molecular diffusion coefficients for bacteriophage MS2 and PRD1 at 15°C are $7.1 \times 10^{-4}$ and $2.8 \times 10^{-4}$ cm$^2$/h, respectively. The tortuosity coefficient for the sand was assumed to be $\tau = 1.43$ (de Marsily 1986).

The appropriate initial and boundary conditions for the transport system examined here are:

$$C(0, z) = C^*(0, z) = C^\diamond(0, z) = 0, \tag{4}$$

$$-D_z\theta_m \frac{\partial C(t, 0)}{\partial z} + q(t, 0)C(t, 0) = \begin{cases} q(t, 0)C_0, & 0 \leq t \leq t_p \\ 0 & t_p \leq t \end{cases}, \tag{5}$$

$$\frac{\partial C(t, \infty)}{\partial z} = 0, \tag{6}$$

where $C_0$ is the pulse-type source concentration, and $t_p$ is the duration of the pulse. The condition (4) establishes that there is no initial liquid phase and adsorbed virus concentrations within the porous medium. The flux-type boundary condition (5) for pulse injection implies concentration discontinuity at the ground surface (inlet) and leads to material balance conservation (Parker and van Genuchten 1984; Chrysikopoulos et al. 1990). The downstream boundary condition (6) preserves concentration continuity for a vertical, semi-infinite porous medium.

3.2 Virus Sorption onto Interfaces

The accumulation of deposited viruses at solid–liquid and air–liquid interfaces is described by the following expressions (Sim and Chrysikopoulos 1999)

$$\rho \frac{\partial C^*}{\partial t} = k\theta_m(C - C_g) - \lambda^*\rho C^*, \tag{7}$$

$$\frac{\partial}{\partial t}(\theta_m C^\diamond) = k^\diamond \theta_m C - \lambda^\diamond \theta_m C^\diamond, \tag{8}$$

where $k$ and $k^\diamond$ are the liquid to liquid–solid and liquid to air–liquid interface mass transfer rate coefficients, respectively; and $C_g(t, z)$ is the liquid phase concentration of viruses in direct contact with solids. It is assumed that the following linear equilibrium relationship is valid (Sim and Chrysikopoulos 1996)

$$C^* = K_d C_g, \tag{9}$$

where $K_d$ is the partition or distribution coefficient and implies that virus sorption onto solids occurs if the liquid phase virus concentration ($C$) is greater than liquid phase virus concentration in direct contact with solids ($C_g$), whereas desorption occurs when $C$ is smaller than $C_g$. As discussed by Sim and Chrysikopoulos (1998), (7) and (9) represent a nonequilibrium virus sorption model with forward rate coefficient equal to $k$ and reverse rate coefficient equal to $k/K_d$. Note that the nonequilibrium virus sorption model employed here is considered appropriate because recent experimental work by Anders and Chrysikopoulos (2005) suggested that the detachment rate coefficients are at least one-order-of-magnitude smaller than the forward rate coefficients for bacteriophage transport in water saturated porous media. However, Sim and Chrysikopoulos (1996, 1998) have shown that the virus transport model presented in this work can easily be modified to account for colloid filtration theory with first-order reversible sorption.

The liquid to liquid–solid interface mass transfer rate coefficient is expressed as:

$$k = \kappa a_T, \tag{10}$$

where $\kappa$ is the liquid to liquid–solid interface mass transfer coefficient; and $a_T$ is the specific liquid–solid interface area. It should be noted that the transfer of viruses from the bulk liquid to a liquid–solid interface is assumed to be governed by virus diffusion through an outer liquid layer surrounding the soil particle, the thickness of which depends on local hydrodynamic conditions (Vilker and Burge 1980; Fogler 1992).

The liquid to liquid–solid interface mass transfer coefficient, $\kappa$, was calculated by defining $a_T$ as the ratio of total surface area of soil particles to the bulk volume of the porous medium (Fogler 1992)

$$a_T = \frac{3(1 - \theta_s)}{r_p} \tag{11}$$

where $r_p$ represents the average radius of soil particles; and $\theta_m = \theta_s$ is the water content of the saturated porous medium.

The liquid to air–liquid interface mass transfer rate coefficient is defined as

$$k^\diamond = \kappa^\diamond a_T^\diamond, \tag{12}$$

where $\kappa^\diamond$ is the liquid to air–liquid interface mass transfer coefficient; and $a_T^\diamond$ is the specific air–liquid interface area.

The capillary tube model presented by Cary (1994), which relies on experimental capillary pressure-saturation relations to estimate the pore-size distribution, was used to calculate the specific air–liquid interface area. This model defines $a_T^\diamond$ as the ratio of the total air–liquid interface area to the bulk volume of the porous medium

$$a_T^\diamond(\theta_m) = \frac{2\theta_s^b}{r_0} \left[ \zeta\theta_r \frac{\theta_s^{-b} - \theta_m^{-b}}{-b} + \frac{\theta_s^{1-b} - \theta_m^{1-b}}{1 - b} \right], \tag{13}$$

where $\zeta$ and $b$ are empirical, soil type specific constants; $\theta_r$ is the monolayer volumetric moisture content; and $r_0$ is the effective pore radius at air-entry which can be evaluated by the capillary rise equation with zero contact angle as follows (Guymon 1994, p. 43):

$$r_0 = \frac{2\sigma}{\rho_{\mathrm{w}} g h_0}, \tag{14}$$

where $\sigma$ is the surface tension of water; $\rho_{\mathrm{w}}$ is the density of water; $g$ is the gravitational constant; and $h_0$ is the air-entry value, defined as the pore water head where air begins to enter water-saturated pores. It should be noted that $a_{\mathrm{T}}^{\diamond}$ is a function of moisture content and takes a value of zero when $\theta_{\mathrm{m}} = \theta_{\mathrm{s}}$. Thus (12) and (13) suggest that the liquid to air–liquid interface mass transfer rate coefficient, $k^{\diamond}$, decreases with increasing moisture content. Consequently, the transfer of viruses at the air–liquid interface is controlled by the moisture content. Furthermore, it should be noted that for a given moisture content the accumulation of viruses at air–liquid interfaces, as described by (8), is assumed to be governed by irreversible virus sorption onto the air–water interface and subsequent virus inactivation. Similar assumption has been considered by other investigators (Zhuang and Jin 2003).

The governing equation for virus transport (1) in conjunction with the relationships (7)–(14) are solved numerically subject to initial and boundary conditions (4)–(6). The numerical solutions are obtained by using appropriate *International Mathematics and Statistics Libraries, Inc.* (1991) one-dimensional partial differential equation solvers.

## 4 Results and Discussion

### 4.1 Transport Parameters

In order to more accurately predict the transport of viruses in saturated and unsaturated porous media using liquid to liquid–solid and liquid to air–liquid interface mass transfer rate coefficients, unfavorable attachment conditions were established in the columns by preparing the bacteriophage/bromide suspension as a low-ionic-strength PBS solution, pH-adjusted to 7.5 (Chu et al. 2001). The phosphate in the virus suspension further minimizes any attachment of viruses by masking the effects of positively charged heterogeneities on virus transport owing to the presence of hematite coatings on the soil grains (Chi and Amy 2004).

A set of four column experiments (two saturated and two unsaturated) were completed using the virus suspension. Shown in Fig. 3 are the normalized bromide concentrations observed for experiment 1 at 100% water saturation (Fig. 3a), experiment 2 at 100% water saturation (Fig. 3b), experiment 3 at 76% water saturation (Fig. 3c) and experiment 4 at 54% water saturation (Fig. 3d). Clearly, the bromide concentration response curves shown in Fig. 3 indicate that there was no bromide retention in the columns. The longer response curves for the unsaturated column experiments were induced by the lower solution flow rates, which were required in order to maintain a constant water potential throughout the packed column.

Shown in Fig. 4 are the normalized bacteriophage MS2 (solid circle) and PRD1 (solid square) observed concentrations for the saturated (Fig. 4a, b) and unsaturated (Fig. 4c–f) column experiments. It should be noted that normalized bacteriophage concentrations over 1 are due to slight variations in the effluent concentrations of each bacteriophage determined by counting the number of plaques on duplicate plates.

All fixed model parameter values for the model simulations are listed in Table 1. The values for the empirical coefficients $\zeta$ and $b$ for sand are adopted from Cary (1994). The value of $h_0$ was obtained by the empirical relationship developed by van Genuchten (1980) to describe the soil water retention curve as:

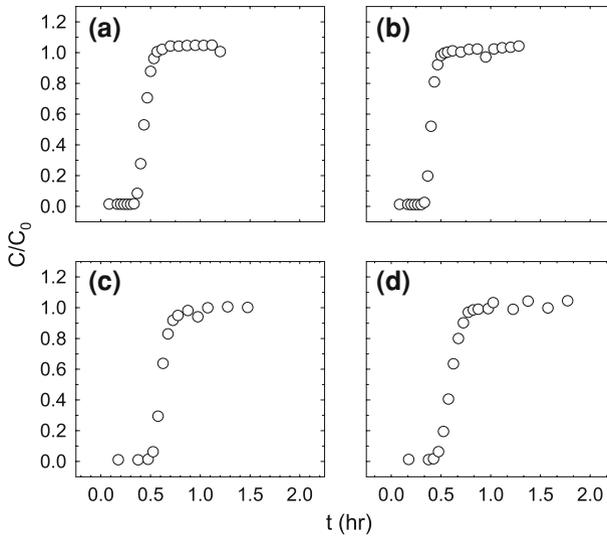$$S_{\mathrm{e}} = \frac{1}{[1 + (\alpha h)^n]^m}, \tag{15}$$

**Fig. 3** Bromide concentration breakthrough data for (**a**) experiment 1 at 100% water saturation, (**b**) experiment 2 at 100% water saturation, (**c**) experiment 3 at 76% water saturation and (**d**) experiment 4 at 54% water saturation

where $S_e$ is the effective degree of saturation, also called the reduced moisture content ($0 \leq S_e \leq 1$); $h$ is the soil moisture pressure head; $\alpha$ is an empirical coefficient whose inverse is equal to the air-entry value, $h_0$; and $n$ and $m$ are empirical constants affecting the shape of the retention curve. Shown in Fig. 5 is the soil retention curve obtained by fitting (15) to the measured retention data representing points along a drainage curve, collected following the procedures outlined by Campbell and Gee (1986). The soil retention curve was generated with use of the hydraulic parameters: $\theta_r = 0.003 \, \text{cm}^3/\text{cm}^3$, $\theta_s = 0.409 \, \text{cm}^3/\text{cm}^3$, $\alpha = 0.0334 \, \text{cm}^{-1}$, $n = 5.781$, and $m = 0.827$.

The virus inactivation rate coefficients $\lambda$, $\lambda^*$, and $\lambda^\diamond$ used to simulate the observed bacteriophage concentrations were obtained from static and dynamic batch experiments conducted to study the effects of temperature and the presence of sand on bacteriophage MS2 and PRD1 inactivation (Anders and Chrysikopoulos 2006). For MS2, the inactivation rate coefficients were $\lambda = 2.5 \times 10^{-3} \, \text{h}^{-1}$; $\lambda^* = 2.75 \times 10^{-3} \, \text{h}^{-1}$; and $\lambda^\diamond = 2.95 \times 10^{-3} \, \text{h}^{-1}$. For PRD1, the $\lambda$, $\lambda^*$, and $\lambda^\diamond$ values were $8.75 \times 10^{-5} \, \text{h}^{-1}$, $8.5 \times 10^{-5} \, \text{h}^{-1}$ and $5.0 \times 10^{-3} \, \text{h}^{-1}$, respectively. It should be noted here that although virus inactivation rate coefficients are time- and temperature-dependent (Sim and Chrysikopoulos 1996; Chrysikopoulos and Vogler 2004), in this study they are assumed to be constant. Furthermore, the experiments were designed to minimize the effect of inactivation by performing the experiments in a constant-temperature room held at 15°C for a period of less than 5 h.

Values of $U$ (pore water velocity defined as $q/\theta_m$) and $D_z$ for each saturated experiment were obtained by fitting the standard advection–dispersion equation to the bromide breakthrough response. Furthermore, the values of $k$ and $K_d$ were obtained by fitting the virus transport model for saturated flow conditions to the observed bacteriophage concentrations by using the previously estimated values of $U$ and $D_z$. The parameter $k^\diamond$ was set to zero because at 100% water saturation there is no air–liquid interfaces present in the packed columns.
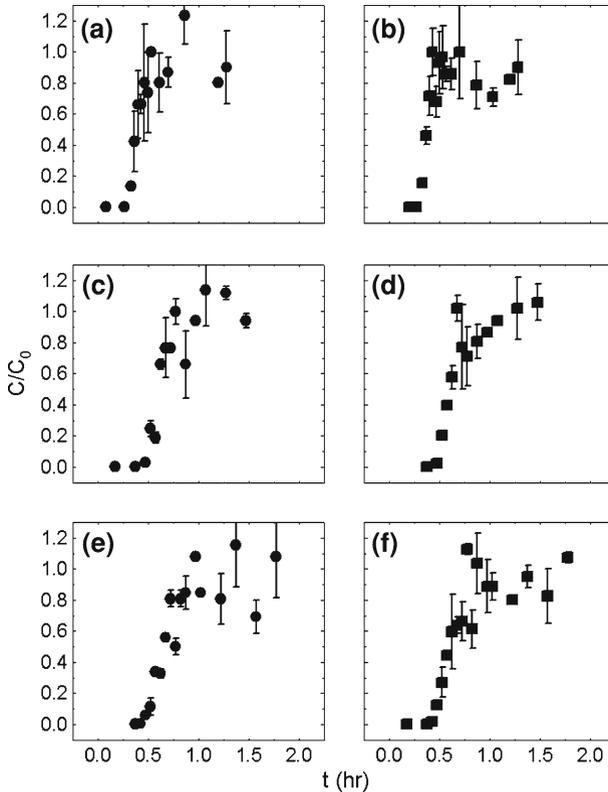
**Fig. 4** Concentration breakthrough data for bacteriophage MS2 (solid circles) and PRD1 (solid squares) at (**a**, **b**) 100% water saturation, (**c**, **d**) 76% water saturation and (**e**, **f**) 54% water saturation. The error bars show the standard deviation associated with the averaged concentration from the plaques counted on duplicate plates

**Table 1** Fixed model parameters for simulations

| Parameter | Value | Units |
|-----------|-------|-------|
| $r_p$ | 0.0125 | cm |
| $\rho$ | 1.65 | $g/cm^3$ |
| $\theta_r$ | 0.003 | $cm^3/cm^3$ |
| $h_0$ | 29.94 | cm |
| $b$ | 2 | – |
| $\zeta$ | 160 | – |
| $\sigma$ | 0.0728 | N/m |
| $g$ | 980 | $cm/s^2$ |

   Water flow in unsaturated or variably saturated, homogeneous, rigid porous media is traditionally described with the Richards equation (Philip 1969; Bear 1972). However, in this study all unsaturated column experiments were conducted only after a constant water potential was achieved throughout the packed column. For constant soil moisture distribution, the unknown values of $U$ and $D_z$ for the unsaturated column experiments were estimated by using the same procedure as described above for the saturated column experiments. The remaining unknown parameters for the unsaturated column experiments, $k$, $K_d$, and $k^\diamond$, were
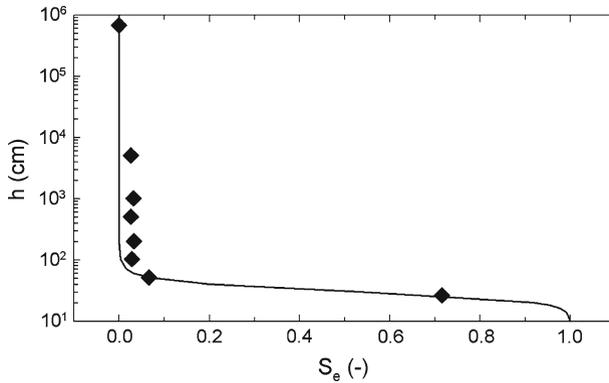
**Fig. 5** Measured retention data (symbols) of the sand used to pack the columns and fitted model (solid curve)

obtained by fitting the virus transport model to the observed bacteriophage breakthrough concentrations.

There are several procedures available in the literature for the estimation of the unknown parameters (Beck and Arnold 1977). In this work the Levenberg–Marquardt nonlinear least squares regression method (Levenberg 1944; Marquardt 1963) is employed. The objective of the nonlinear least squares method is to calculate values of the model parameters that minimize the residual sum of squared error (SSE) between simulated and observed data.

4.2 Model Simulations

Model transport parameters and SSE corresponding to the experimental data for bacteriophage MS2 and PRD1 during the saturated and unsaturated column experiments are listed in Table 2. It should be noted that the slightly different $a_T$ values, obtained from (11), are due to differences in porosity of the column that occurred by reassembling the column apparatus between experiments. Values of $a_T^\diamond$, calculated from (13), increased from 95.3 to 311.1 cm$^{-1}$ as the water saturation level was reduced from 76 to 54%. These specific air–liquid interface areas, $a_T^\diamond$, indicate that the saturation levels achieved during the experiments conducted in this study never exceeded the effective water film thickness necessary to produce film straining of bacteriophage MS2 or PRD1. The water film thickness is given by the ratio of the bulk volume of the porous medium to the total air–liquid interface area (averaged over both true water thickness and pendular water around grain–grain contacts) (Wan and Tokunaga 1998).

Shown in Fig. 6 are the model simulated bacteriophage MS2 concentration history curves (solid curves) as a function of pore volume for the saturated (Fig. 6a) and unsaturated (Fig. 6b, c) column experiments. The estimated values of $K_d$ for bacteriophage MS2 varied from 33.72 cm$^3$/g at 100% water saturation to 380.9 cm$^3$/g at 76% water saturation, with an intermediate value of 136.7 at 54% water saturation. The range of $K_d$ values suggests that a reduction in soil moisture content can enhance virus sorption by allowing viruses to partition more strongly onto soil particles.

The estimated parameter $k$ increased from $3.7 \times 10^{-4}$ h$^{-1}$ at 100% water saturation to $3.3 \times 10^{-3}$ h$^{-1}$ at 76% water saturation, and increased further to $7.6 \times 10^{-3}$ h$^{-1}$ at 54% water saturation. Using the $K_d$ and $k$ values for bacteriophage MS2 at 100, 76, and 54% water

**Table 2** Model parameters corresponding to the experimental data for bacteriophage MS2 and PRD1

| Parameter | Exp 1 100% | Exp 2 | Exp 3 76% | Exp 4 54% | Units |
|---|---|---|---|---|---|
| $\theta_s$ | 0.41 | 0.40 | 0.42 | 0.37 | $cm^3/cm^3$ |
| $\theta_m$ | – | – | 0.32 | 0.20 | $cm^3/cm^3$ |
| $U$ | 37.8 | 41.4 | 24.6 | 25.2 | cm/h |
| $D_z$ | 5.46 | 2.92 | 2.20 | 4.27 | $cm^2/h$ |
| $a_T$ | 141.6 | 144.0 | 139.2 | 151.2 | $cm^{-1}$ |
| $a_T^\diamond$ | – | – | 95.3 | 311.1 | $cm^{-1}$ |
| MS2 | | | | | |
| $k$ | $3.7\times10^{-4}$ | – | $3.3\times10^{-3}$ | $7.6\times10^{-3}$ | $h^{-1}$ |
| $K_d$ | 33.72 | – | 380.9 | 136.7 | $cm^3/g$ |
| $k^\diamond$ | – | – | 0.012 | 0.18 | $h^{-1}$ |
| SSE | 1.32 | – | 0.20 | 0.34 | – |
| PRD1 | | | | | |
| $k$ | – | $3.2\times10^{-5}$ | $1.6\times10^{-3}$ | 0.012 | $h^{-1}$ |
| $K_d$ | – | 36.17 | 311.9 | 40.75 | $cm^3/g$ |
| $k^\diamond$ | – | – | $3.5\times10^{-3}$ | 0.10 | $h^{-1}$ |
| SSE | – | 0.30 | 0.20 | 0.24 | – |

saturation, the detachment rate coefficients are estimated to be: $1.1 \times 10^{-5}$, $8.7\times10^{-6}$, and $5.6 \times 10^{-5}$ g/cm$^3$ h, respectively. It should be noted here that detachment rate coefficient is given by the ratio $k/K_d$ (Sim and Chrysikopoulos 1998).

The estimated $k^\diamond$ value at 76% water saturation is $0.012\,h^{-1}$ and increased to $0.18\,h^{-1}$ at 54% water saturation. The estimated $k$ and $k^\diamond$ values for bacteriophage MS2 at 76 and 54% water saturation suggest that the bacteriophage are sorbed more strongly onto air–liquid interfaces than onto liquid–solid interfaces. Studies indicating that colloidal particles are sorbed more strongly onto air–liquid interfaces than onto liquid–solid interfaces have also been reported by other investigators (Wan and Wilson 1994).
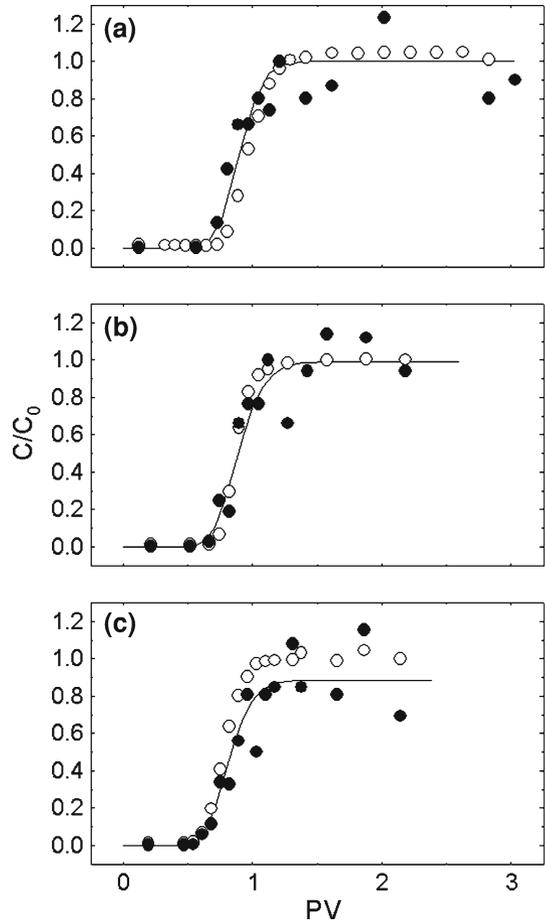
Shown in Fig. 7 are the model simulated bacteriophage PRD1 concentration history curves (solid curves) as a function of pore volume for the saturated (Fig. 7a) and unsaturated (Fig. 7b, c) column experiments. The estimated values of $K_d$ for bacteriophage PRD1 ranged from 36.17 cm$^3$/g at 100% water saturation to 311.9 cm$^3$/g at 76% water saturation. This result confirms that partitioning of viruses onto liquid–solid interfaces is significant under the conditions of the unsaturated column experiments of this study, but the relationship between the degree of water saturation and $K_d$ is not clear and requires further investigation.

The estimated parameter $k$ increased from $3.2 \times 10^{-5}\,h^{-1}$ at 100% saturation to $1.6 \times 10^{-3}\,h^{-1}$ at 76% water saturation and increased further to $0.012\,h^{-1}$ at 54% water saturation. Using the $K_d$ and $k$ values for bacteriophage PRD1, estimated detachment rates increased from $8.8 \times 10^{-7}$ g/cm$^3$ h at 100% water saturation to $5.1 \times 10^{-6}$ g/cm$^3$ h at 76% water saturation, and increased further to $2.9 \times 10^{-4}$ g/cm$^3$h at 54% water saturation. The estimated $k^\diamond$ values increased from $3.5 \times 10^{-3}\,h^{-1}$ at 76% water saturation to $0.10\,h^{-1}$ at 54% water saturation; these values are smaller than the $k^\diamond$ values estimated for bacteriophage MS2 for the same water saturation levels.

### 4.3 Air–Liquid–Solid Interface Mass Transfer Coefficients

Figure 8 shows the calculated liquid to liquid–solid and liquid to air–liquid interface mass transfer coefficients for bacteriophage MS2 and PRD1 by employing (10) and (12) and the
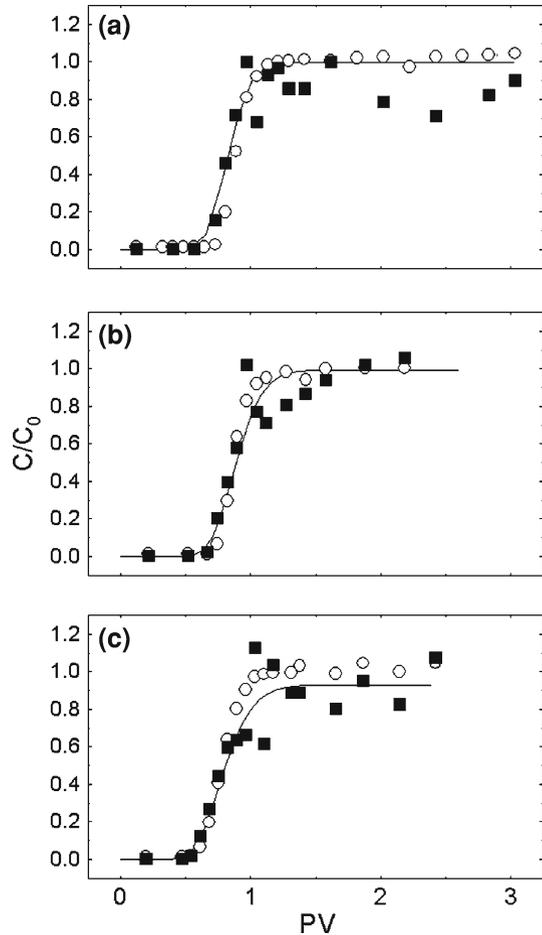
**Fig. 6** Simulated concentration histories (solid curves) for bacteriophage MS2 at (**a**) 100% water saturation, (**b**) 76% water saturation and (**c**) 54% water saturation. Also shown are corresponding bromide (open circles) and bacteriophage MS2 (solid squares) concentration breakthrough data



parameters listed in Table 2. For bacteriophage MS2, shown in Fig. 8a, values of $\kappa$ increased from $2.6 \times 10^{-6}$ to $5.0 \times 10^{-5}$ cm/h as the water saturation is reduced to 54% even as the $a_T$ values are only slightly different throughout the saturated and unsaturated experiments. The $\kappa^{\diamond}$ values increase from $1.2 \times 10^{-4}$ to $6.0 \times 10^{-4}$ cm/h. Therefore, the reduction in water saturation has the effect of increasing both $\kappa^{\diamond}$ and $\kappa$. The calculated value of $\kappa^{\diamond}$ is approximately five times larger than the one for $\kappa$ at 76% water saturation, and about 12 times larger at 54% water saturation. The observed increase in the $\kappa^{\diamond}$ to $\kappa$ ratio confirms that bacteriophage MS2 are sorbed more strongly onto air–liquid interfaces than onto liquid–solid interfaces. This phenomenon provides a plausible explanation for the rapid removal of viruses observed during periods of minor changes of water saturation levels in porous media during artificial recharge (Anders et al. 2004).
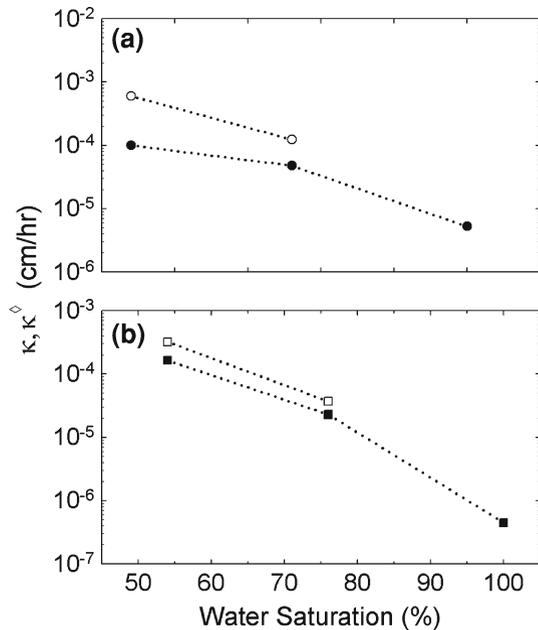
For bacteriophage PRD1, $\kappa$ values shown in Fig. 8b increase from $2.2 \times 10^{-7}$ to $8.2 \times 10^{-5}$ cm/h and $\kappa^{\diamond}$ values increase from $3.7 \times 10^{-5}$ to $3.2 \times 10^{-4}$ cm/h as water saturation levels are reduced from 76 to 54%. These $\kappa$ and $\kappa^{\diamond}$ values are slightly smaller than the corresponding parameter values for bacteriophage MS2. PRD1 exhibits a calculated $\kappa^{\diamond}$ to $\kappa$ ratio of 3 and 4 at 76 and 54% water saturation, respectively.

Although previous studies have suggested that attachment of viruses to liquid–solid and air–liquid interfaces is increasing with decreasing water saturation levels due to a more pronounced effect of electrostatic and hydrophobic interactions, such an effect was minimized in this study by establishing unfavorable attachment conditions within the sand columns (e.g., phosphate-buffered solution; pH = 7.5; ionic strength = 2 mM). Another possible explanation for the greater influence of saturation levels on the increased attachment of viruses, especially for bacteriophage MS2, is the reduction in the diffusion length within the pores at lower saturations combined with changes in the specific liquid–solid and air–liquid interface areas. In this study, the water potential was held constant throughout each saturated and unsaturated column experiment. However, if water saturation levels decrease during the unsaturated experiments, the damage to specific bacteriophage PRD1 and MS2 viral components related to infection is expected to increase due to the presence of greater air–liquid interfaces (Anders and Chrysikopoulos 2006), which subsequently leads to a reduction in effluent virus concentrations.

**Fig. 8** Calculated values of liquid to liquid–solid interface mass transfer coefficients (solid symbols) and liquid to air–liquid interface mass transfer coefficients (open symbols) for bacteriophage (**a**) MS2 and (**b**) PRD1



## 5 Summary

Laboratory-scale transport experiments were conducted in packed sand columns under saturated and unsaturated conditions using the male-specific RNA coliphage, MS2 and the *Salmonella typhimurium* phage, PRD1 as model viruses. Liquid to liquid–solid and liquid to air–liquid interface mass transfer rate coefficients were obtained by fitting a previously developed virus transport model to the experimental data. The estimated liquid to liquid–solid and liquid to air–liquid interface mass transfer rates increased for both bacteriophage as water saturation levels were reduced from 100 to 54%. It was observed that bacteriophage MS2 sorbed more strongly onto air–liquid interfaces than onto liquid–solid interfaces. For bacteriophage PRD1 it is the combination of several processes that contribute to the lower effluent concentrations at 54% water saturation. Therefore, even under unfavorable attachment conditions within a sand column (e.g., phosphate-buffered solution; $pH = 7.5$; ionic strength $= 2\,mM$), water saturation fluctuations can affect virus transport through porous media.

## References

Anders, R., Chrysikopoulos, C.V.: Virus fate and transport during artificial recharge with recycled water. Water Resour. Res. **41**, W10415 (2005). doi:10.1029/2004-WR003419
Anders, R., Chrysikopoulos, C.V.: Evaluation of the factors controlling the time-dependent inactivation rate coefficients of bacteriophage MS2 and PRD1. Environ. Sci. Techol. **40**(10), 3237–3242 (2006)

Anders, R., Yanko, W.A., Schroeder, R.A., Jackson, J.L.: Virus Fate and Transport During Recharge Using Recycled Water at a Research Field Site in the Montebello Forebay, Los Angeles County, CA, 1997–2000. U.S. Geological Survey Scientific Investigation Report 2004–5161, p. 65 (2004)

Atkins, P.W.: Physical Chemistry, 4th edn., 995 pp. Oxford University Press, New York (1990)

Bales, R.C., Hinkle, S.R., Kroeger, T.W., Stockling, K., Gerba, C.P.: Bacteriophage adsorption during transport through porous media: chemical perturbations and reversibility. Environ. Sci. Technol. **25**(12), 2088–2095 (1991)

Bales, R.C., Li, S., Yeh, T.C.J., Lenczewski, M.E., Gerba, C.P.: Bacteriophage and microscope transport in saturated porous media: forced-gradient experiment at Bordon, Ontario. Water Resour. Res. **33**(4), 639–648 (1997)

Bear, L.: Dynamics of Fluids in Porous Media. Dover, Mineola, NY (1972)

Beck, J.V., Arnold, K.J.: Parameter Estimation in Engineering and Science. Wiley, NY (1977)

Campbell, G.S., Gee, G.W.: Water potential—miscellaneous methods. In: Klute, A. (ed.) Methods of Soil Analysis, Part 1 (2nd edn.), pp. 625–628 (1986)

Cary, J.W.: Estimating the surface area of fluid phase interfaces in porous media. J. Contam. Hydrol. **15**, 243–248 (1994)

Chi, F.H., Amy, G.L.: Kinetic study on the sorption of dissolved natural organic matter onto different aquifer materials: the effects of hydrophobicity and functional groups. J. Colloid Interface Sci. **274**(2), 380–391 (2004)

Chrysikopoulos, C.V.: Artificial tracers for geothermal reservoir studies. Environ. Geol. **22**, 60–70 (1993)

Chrysikopoulos, C.V., Roberts, P.V., Kitanidis, P.K.: One-dimensional solute transport in porous media with partial well-to-well recirculation: application to field experiments. Water Resour. Res. **26**(6), 1189–1195 (1990)

Chrysikopoulos, C.V., Sim, Y.: One-dimensional virus transport in homogeneous porous media with time dependent distribution coefficient. J. Hydrol. **185**, 199–219 (1996)

Chrysikopoulos, C.V., Vogler, E.T.: Estimation of time dependent virus inactivation rates by geostatistical and resampling techniques: application to virus transport in porous media. Stochastic Environ. Res. Risk Assess. **18**(2), 67–78 (2004)

Chu, Y., Jin, Y., Flury, M., Yates, M.V.: Mechanisms of virus removal during transport in unsaturated porous media. Water Resour. Res. **37**(2), 253–263 (2001)

Clark, R.N., Swayze, G.A., Wise, R., Livo, E., Hoefen, T., Kokaly, R., Sutley, S.J.: USGS digital spectral library splib06a. U.S. Geological Survey. Digital Data Series 231. http://speclab.cr.usgs.gov/spectral.lib06 (2007)

Debartolomeis, J., Cabelli, V.J.: Evaluation of an *Escherichia coli* host strain for enumeration of male-specific bacteriophages. Appl. Environ. Microb. **57**, 1301–1305 (1991)

de Marsily, G.: Quantitative Hydrogeology. Groundwater Hydrology for Engineers, 440 pp. Academic Press, San Diego, CA (1986)

Fogler, H.S.: Elements of Chemical Reaction Engineering, 2nd edn. Prentice Hall (1992)

Gerba, C.P.: Applied and theoretical aspects of virus adsorption to surfaces. Adv. Appl. Microb. **30**, 133–168 (1984)

Gerba, C.P., Keswick, B.H.: Survival and transport of enteric bacteria and viruses in groundwater. Stud. Environ. Sci. **17**, 511–515 (1981)

Guymon G.L.: Unsaturated Zone Hydrology. Prentice Hall (1994)

Harvey, R.W., Ryan, J.N.: Use of PRD1 bacteriophage in groundwater viral transport, inactivation, and attachment studies. FEMS Microbiol. Ecol. **49**, 3–16 (2004)

Hurst, C.J., Gerba, C.P., Cech, I.: Effects of environmental variables and soil characteristics on virus survival in soil. Appl. Environ. Microb. **40**, 1067–1079 (1980)

International Mathematics and Statistics Libraries, Inc.: IMSL MATH/LIBRARY User's Manual, ver. 2.0. Houston, TX (1991)

Jin, Y., Chu, Y., Li, Y.: Virus removal and transport in saturated and unsaturated sand columns. J. Contam. Hydrol. **43**, 111–128 (2000)

Keller, A.A., Sirivithayapakorn, S., Chrysikopoulos, C.V.: Early breakthrough of colloids and bacteriophage MS2 in a water-saturated sand column. Water Resour. Res. **40**(8), W08304 (2004). doi:1029/2003WR002676

Lance, J.C., Gerba, C.P.: Virus movement in soil during saturated and unsaturated flow. Appl. Environ. Microb. **47**(2), 335–337 (1984)

Levenberg, K.A.: Method for the solution of certain nonlinear problems in least squares. Quart. Appl. Math. **2**, 164–168 (1944)

Marquardt, D.W.: An algorithm for least-squares estimation of nonlinear parameters. SIAM J. Appl. Math. **11**(2), 431–441 (1963)

Masciopinto, C., La Mantia, R., Chrysikopoulos, C.V.: Fate and transport of pathogens in a fractured aquifer in the Salento area, Italy. Water Resour. Res. **41**(10), 44, W01404 (2008). doi:10.1029/2006WR005643

National Research Council: Ground Water Recharge Using Waters of Impaired Quality. National Academy Press, Washington D.C. (1994)

Nielsen, D.R., van Genuchten, M.T., Biggar, J.W.: Water flow and solute transport processes in the unsaturated zone. Water Resour. Res. **22**(9), 89S–108S (1986)

Parker, J.C., van Genuchten, M.T.: Flux-averaged and volume-averaged concentrations in continuum approaches to solute transport. Water Resour. Res. **20**(7), 866–872 (1984)

Philip, J.R: The theory of infiltration. In: Chow, V.T. (ed.) Advances in Hydroscience, vol. 5, pp. 215–296. Academic, San Diego, CA (1969)

Powelson, D.K., Simpson, J.R., Gerba, C.P.: Virus transport and survival in saturated and unsaturated flow through soil columns. J. Environ. Qual. **19**, 396–401 (1990)

Ryan, J.N., Elimelech, E., Ard, R.A., Harvey, R.W., Johnson, P.R.: Bacteriophage PRD1 and silica colloid transport and recovery in an ironoxide-coated sand aquifer. Environ. Sci. Tech. **33**, 63–73 (1999)

Ryan, J.N., Harvey, R.W., Metge, D., Elimelech, M., Navigato, T., Pieper, A.P.: Field and laboratory investigations of inactivation of viruses (PRD1 and MS2) attached to iron oxide-coated quartz sand. Environ. Sci. Technol. **36**, 2403–2413 (2002)

Schijven, J.K., Hoogenboezem, W., Hassanizadeh, S.M., Peters, J.H.: Modeling removal of bacteriophages MS2 and PRD1 by dune recharge at Castricum, Netherlands. Water Resour. Res. **35**, 1101–1111 (1999)

Sim, Y., Chrysikopoulos, C.V.: Analytical models for one-dimensional virus transport in saturated porous media. Water Resour. Res. **31**, 1429–1437 (1995). (Correction, Water Resour. Res. **32**, 1473, (1996))

Sim, Y., Chrysikopoulos, C.V.: One-dimensional virus transport in porous media with time-dependent inactivation rate coefficients. Water Resour. Res. **32**, 2607–2611 (1996)

Sim, Y., Chrysikopoulos, C.V.: Three-dimensional analytical models for virus transport in saturated porous media. Transp. Porous Med. **30**(1), 87–112 (1998)

Sim, Y., Chrysikopoulos, C.V.: Analytical models for virus adsorption and inactivation in unsaturated porous media. Colloids Surf. A: Physicochem. Eng. Asp. **155**(4), 189–199 (1999)

Sim, Y., Chrysikopoulos, C.V.: Virus transport in unsaturated porous media. Water Resour. Res. **36**(1), 173–179 (2000)

Taggart, J.E., Jr. (ed.): Analytical methods for chemical analysis of geologic and other materials: U.S. Geological Survey Open-File Report 02-0223. http://pubs.usgs.gov/of/2002/ofr-02-0223 (2002)

Thompson, S.S., Yates, M.V.: Bacteriophage inactivation at the air–water–solid interface in dynamic batch systems. Appl. Environ. Microb. **65**(3), 1186–1190 (1999)

Thompson, S.S., Flury, M., Yates, M.V., Jury, W.A.: Role of air–water interface in bacteriophage sorption experiments. Appl. Environ. Microb. **64**(1), 304–309 (1998)

U.S. Environmental Protection Agency: Method 1602: Male-specific (F+) and somatic coliphage in water by single agar layer (SAL) procedure. Office of Water, Washington D.C., EPA 821-R-01-029 (2001)

van Genuchten, M.T.: A closed form equation for predicting the hydraulic conductivity of unsaturated soils. Soil Sci. Soc. Am. J. **44**(5), 892–898 (1980)

Vilker, V.L., Burge, W.D.: Adsorption mass transfer model for virus transfer in soils. Water Res. **14**, 783–790 (1980)

Wan, J., Tokunaga, T.K.: Measuring partition coefficients of colloids at air–water interfaces. Environ. Sci. Technol. **32**, 3293–3298 (1998)

Wan, J., Wilson, J.L.: Colloid transport in unsaturated porous media. Water Resour. Res. **30**(4), 857–864 (1994)

Yahya, M.T., Galsomies, L., Gerba, C.P., Bales, R.C.: Survival of bacteriophage MS-2 and PRD-1 in ground water. Water Sci. Technol. **27**, 409–412 (1993)

Yates, M.V., Gerba, C.P., Kelly, L.M.: Virus persistence in groundwater. Appl. Environ. Microb. **49**, 778–781 (1985)

Zerda K.S.: Adsorption of viruses to charge-modified silica. Ph.D. dissertation. Department of Virology and Epidemiology, Baylor College of Medicine, Houston (1982)

Zhuang, J., Jin, Y.: Virus retention and transport through Al-oxide coated sand columns: effects of ionic strength and composition. J Contam. Hydrol. **60**, 193–209 (2003)